THE PASCHEN-BACK EFFECT OF HYPERFINE STRUCTURE II. Bi II AND Bi III

By J. B. Green* and John Wulff†
Mendenhall Laboratory of Physics and Massachusetts Institute of Technology.

(Received September 10, 1931)

Abstract

Goudsmit and Bacher's theory is successfully applied to the spectra of Bi II and Bi III. The lines λλ5719 of Bi II and 4561 and 3695 of Bi III are used as typical examples of these spectra. λ5719, like 3092 of Ti II, serves as an excellent check on the theory, because of its especially simple transition.

IN A previous paper, the authors showed that Goudsmit and Bacher's[1] theory is quite adequate to explain the complicated Zeeman patterns observed for the hyperfine structure components of the spectra of Tl II and Tl III. The present paper is a continuation of the work and treats the spectra of Bi II and Bi III.

The experimental arrangement was exactly the same as in the previous

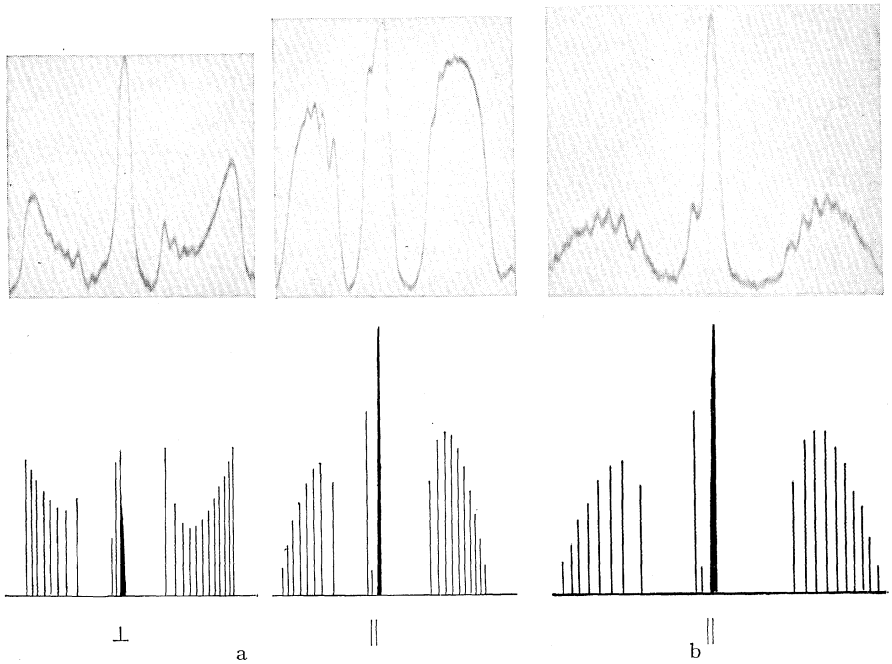

Fig. 1. (a). λ5719 Bi II 14700 gauss second order. (b). λ5719 Bi II 14700 gauss third order

* John Simon Guggenheim Memorial Fellow.
† International Education Board Fellow.
[1] Goudsmit and Bacher, Zeits. f. Physik **66,** 13 (1930).

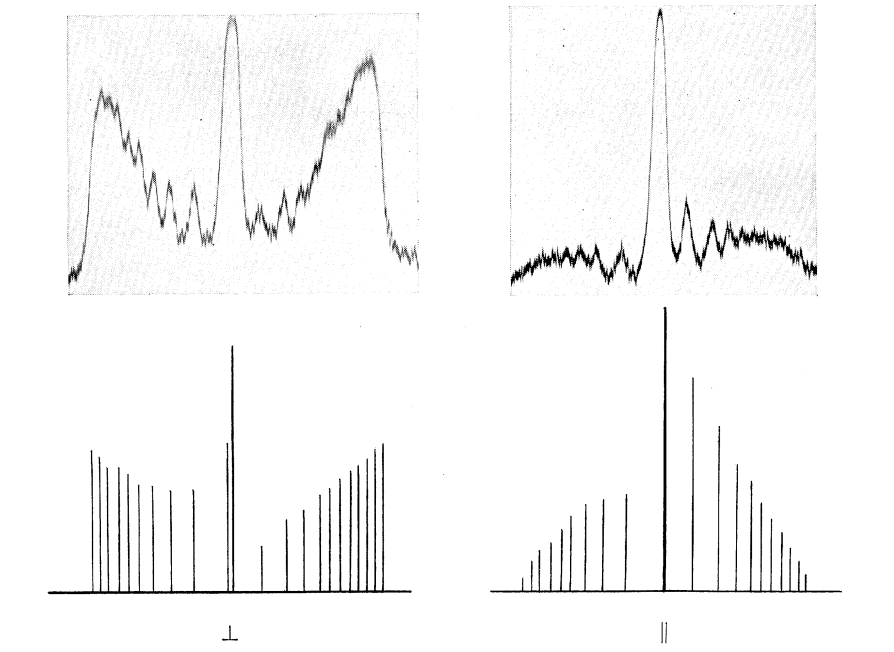

c

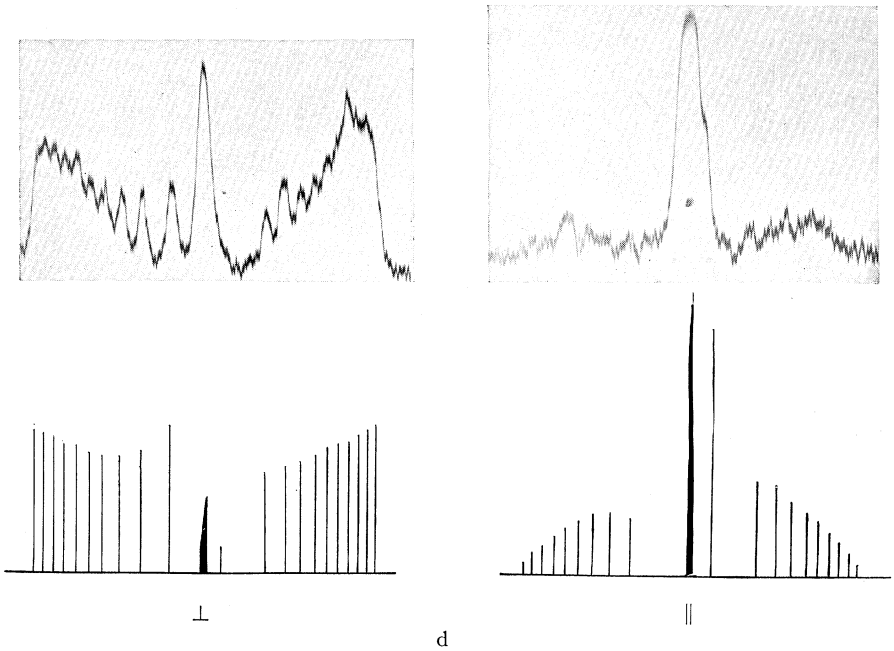

d

Fig. 1. (c). λ5719 Bi II 32500 gauss second order. (d). λ5719 Bi II 43350 gauss second order.

work, except that the thallium metal used on the positive electrode was replaced by pure bismuth metal. For the excitation of spark spectra, alloys of the metal did not prove at all satisfactory. It seems that large quantities of the metallic vapor must be present in order to bring out the spark lines; a condition that must be avoided in the study of arc lines, for it leads almost certainly to self-reversal of some of the components of the lines.

In all other respects too, it was necessary to pay strict attention to all the details. As may be seen from the microphotometer reproductions, the magnetic patterns of the lines are extremely complicated, and in order to prevent the groups of lines from becoming mere smears, the pressure on the vacuum chamber, the current in the arc, and the speed of the motor, had to be kept constant.

Flieger plates of the Perutz Company in Munich were again used, and long tank development with Perutz fine-grain developer served to bring out to the best advantage the really fine work that the grating is capable of doing.

The results of Back and Goudsmit,[2] and Back and Wulff[3] have shown conclusively that the nuclear moment of the bismuth atom is 9/2. Consequently, the Zeeman patterns of the bismuth lines are considerably more complicated than the thallium lines, for in the latter cases, the tendency of each Zeeman component was break up into two in strong magnetic fields, while in the latter, the tendency is to break up into ten!

In the theoretical calculations it would also be possible for the determinantal equation to be of the tenth order and the tedium of the solution of the problem would be enormous, unless one used approximate methods as suggested by Goudsmit and Back. We have therefore chosen a particularly simple type of transition in Bi II to illustrate the theory. The line λ5719 has been classified as $2_1{}^0-7_0$ (possibly $6p\ 7s\,{}^3P_1-6p\ 7p\,{}^3P_0$). We are thus dealing with a transition $j=1$ to $j=0$, exactly similar to λ3092 of Tl II. A glance at Eq. (2) of the previous paper shows that the determinantal equation will be of the third order. There is one further complication in the calculations for Bi II. This is a two-electron spectrum, and the coupling between the electrons is practically *jj* in type. Hence we cannot use the Landé *g*-value in our equations. Applying Houston's[4] theory to the case, we are able to calculate the *g*-values from the interval separations and for $6p\ 7s\ {}^3P_1$ we find the value $g=1.35$ instead of 1.50, the Landé *g*-value. With this value, the agreement between theory and experient was excellent.

The results of the calculations are shown graphically in Figs. 1a,b,c,d. Fig. 1a is taken at a field strength of 14700 gauss in the second order. Above is the microphotometric reproduction of the original plate (13× enlarged), and below the calculated positions and intensities of the lines. Fig. 1b is a reproduction of the third order, parallel polarization. Figs. 1c and 1d were taken from second order plates with magnetic fields of 32500 and 43350 gauss respectively. The wide black lines indicate a large number of very close com-

[2] Back and Goudsmit, Zeits. f. Physik **47,** 174 (1928).
[3] Back and Wulff, Zeits. f. Physik **66,** 31 (1930).
[4] Houston, Phys. Rev. **33,** 297 (1929).

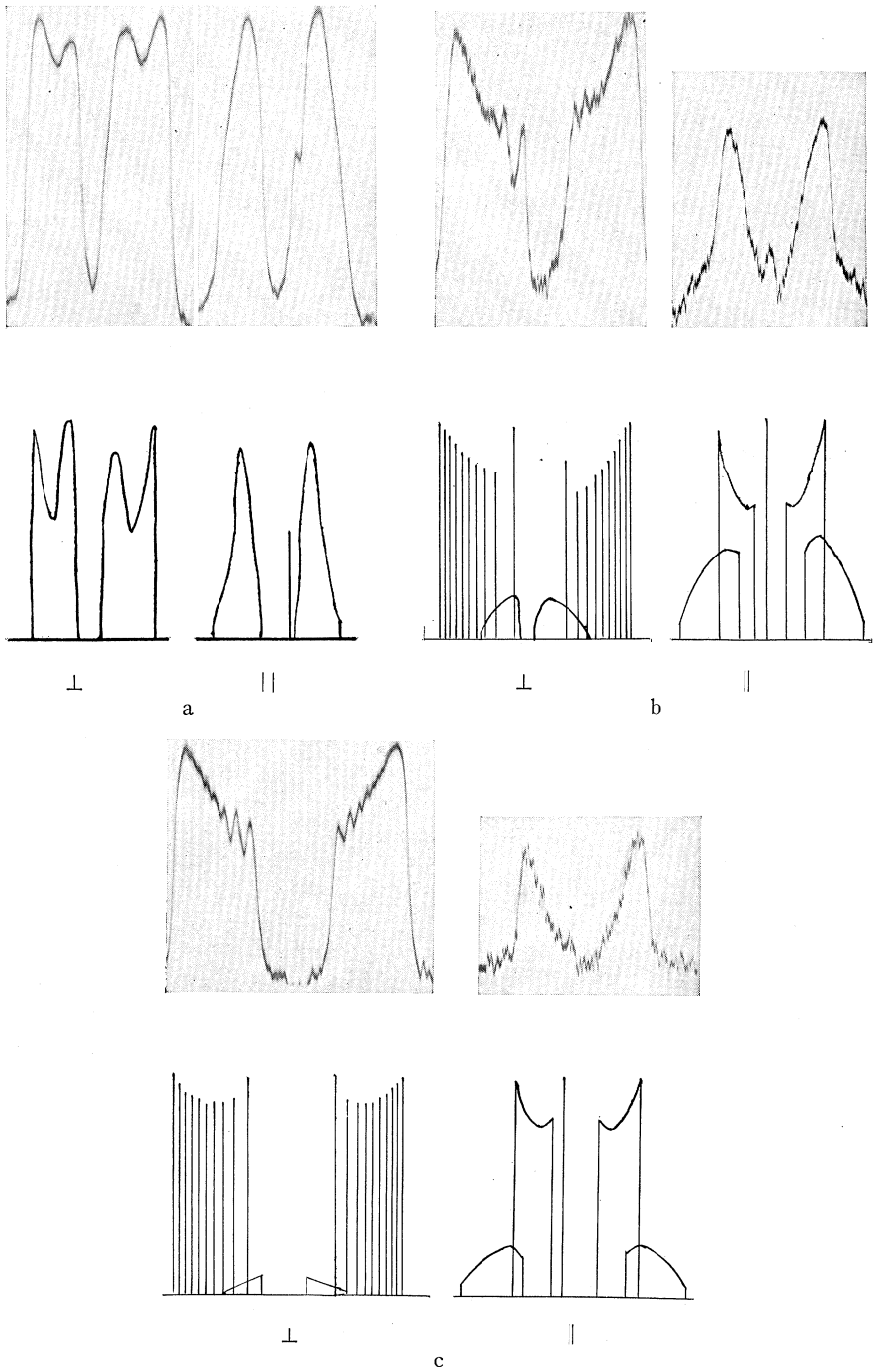

Fig. 2. (a). λ4561 Bi III 14700 gauss second order. (b). λ4561 Bi III 32500 gauss second order. (c). λ4561 Bi III 43350 gauss second order.

ponents and in Fig. 1d, parallel polarization, although these are relatively weak, the grating has integrated their intensities and shows them as one strong line. It is to be noted that the side components in the parallel polarization de-

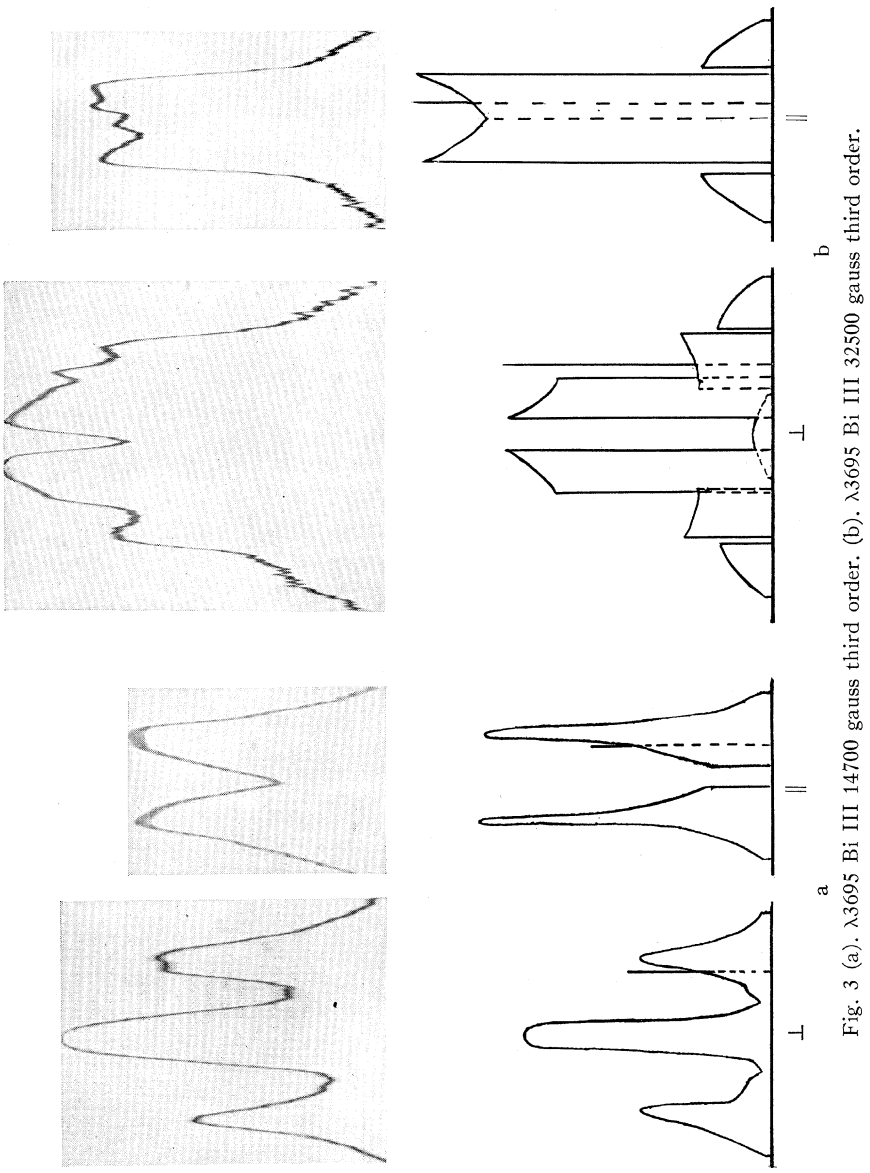

Fig. 3 (a). λ3695 Bi III 14700 gauss third order. (b). λ3695 Bi III 32500 gauss third order.

crease in intensity with increasing field strength, while the outside perpendicular components increase in intensity with increasing field strength. The side parallel components at 43350 gauss are barely perceptible on the photographic plate and their positions are very difficult to determine on the microphotometer record.

As representative lines in the spectrum of Bi III, we chose λλ4561 and 3695. These lines represent the transitions $7s^2S_{1/2}-7p^2P_{1/2}$ and $7s^2S_{1/2}-7p^2P_{3/2}$. These lines were also observed at the three field strengths used in the previous work, namely 14700, 32500 and 43350 gauss, and are represented in Figs. 2a, b,c and 3a b,c respectively.

λ 4561 in strong fields was completely resolved in the perpendicular polarization in the second order, as can be seen on the microphotometer record.

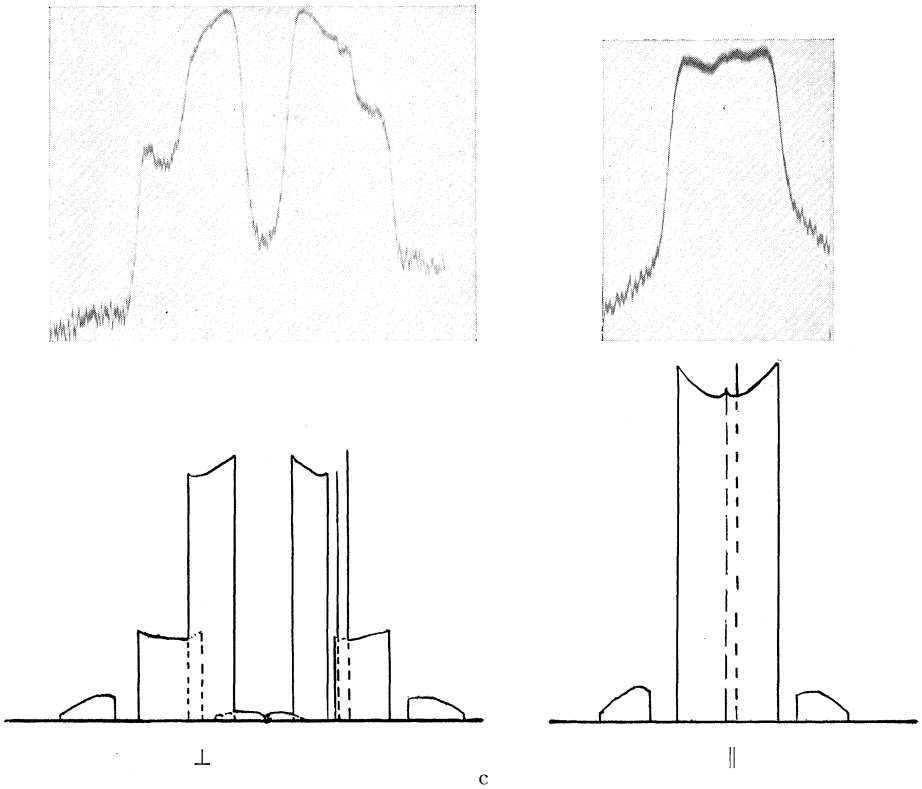

c

Fig. 3 (c). λ3695 Bi III 43350 gauss third order.

In the parallel components, the thing of interest to be noted is that the component marked with an arrow, the only resolvable component in this polarization, moves from the long wave-length group to the short wave-length group as the field strength increases, in complete accordance with the theory. The broad blocks on the computed patterns indicate groups of lines possibly resolvable by the grating but not by the phtographic plate. Fig. 2c shows the result of broadening the photometer slit. The parallel components were recorded with a very fine slit and show plate grain very noticably, while the perpendicular components were recorded with a wider slit, and the plate grain is hardly apparent, but the real breaks in the curve are also reduced so that in some cases they are barely perceptible.

Figs. 3a, b, c represent the results for λ3695 in the third order. The hyperfine separation of the $^2P_{3/2}$ term as given by Fisher and Goudsmit is very small, so that for this term, the approximate formula

$$E = m_j g\omega + A m_i m_j$$

sufficed to determine the energy levels. Here again, in the computed patterns, the blocks represent unresolved groups of lines. When a line sufficiently strong and separated from a group can be seen on the photometer curve, its position is also shown on the theoretical pattern. Unfortunately, the photometer curves are not nearly so rich as the patterns that could be observed with the eye. For example, in the perpendicular polarization for the strong field four sharp lines could easily be distinguished on the long wave-length side of the pattern, while only two show on the photometer curve; and three lines of the corresponding group on the short wave-length side could be separated from the pattern, while none appear on the photometer records. For the low field strength, the blocks on the theoretical pictures overlapped so badly that a sum curve was built and that is the one represented in the figure. This was also done for λ4561. The transition of one line in the parallel polarization from one side of the figure to the other is also noted here.

Here again, then, as in the case of Tl II and Tl III the present status of the theory of the Paschen-Back effect for hyperfine structure is verified in all of its details.

In concluding this work, it gives us great pleasure to acknowledge our thanks to Professors Geiger and Back for the privilege of working at Tübingen, and to the Rockfeller and Guggenheim Foundations for their financial assistance.

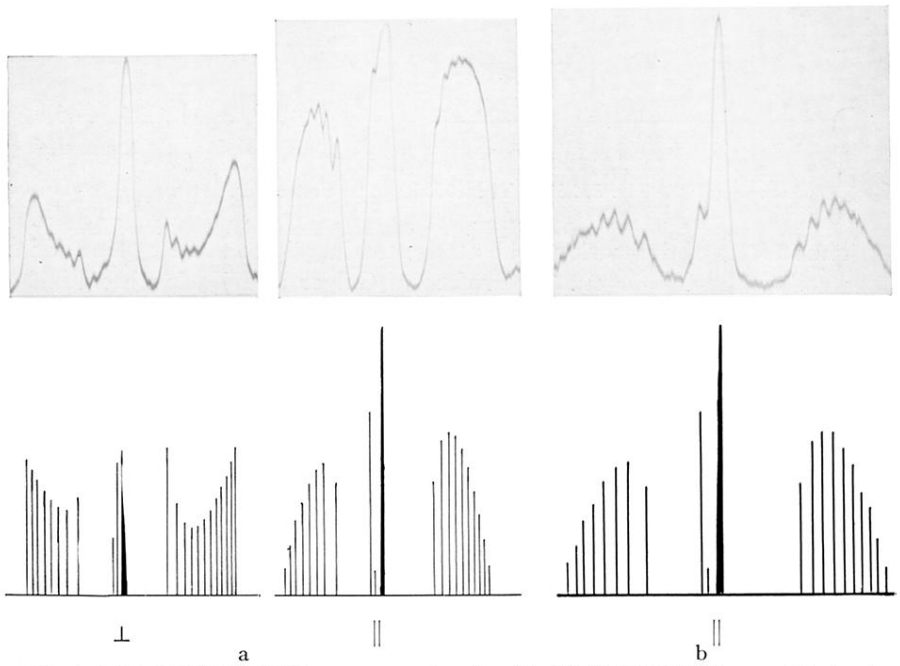

Fig. 1. (a). λ5719 Bi II 14700 gauss second order. (b). λ5719 Bi II 14700 gauss third order

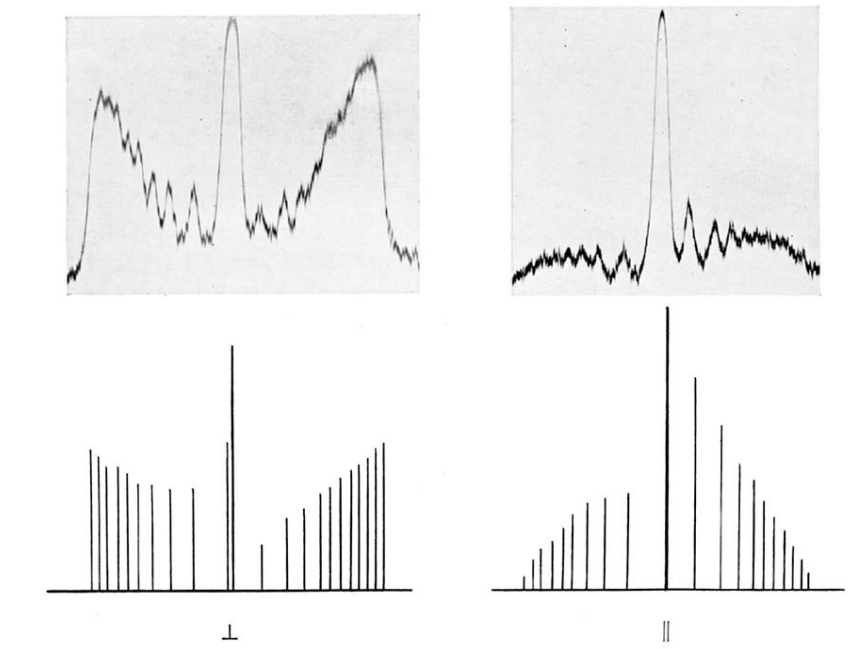

c

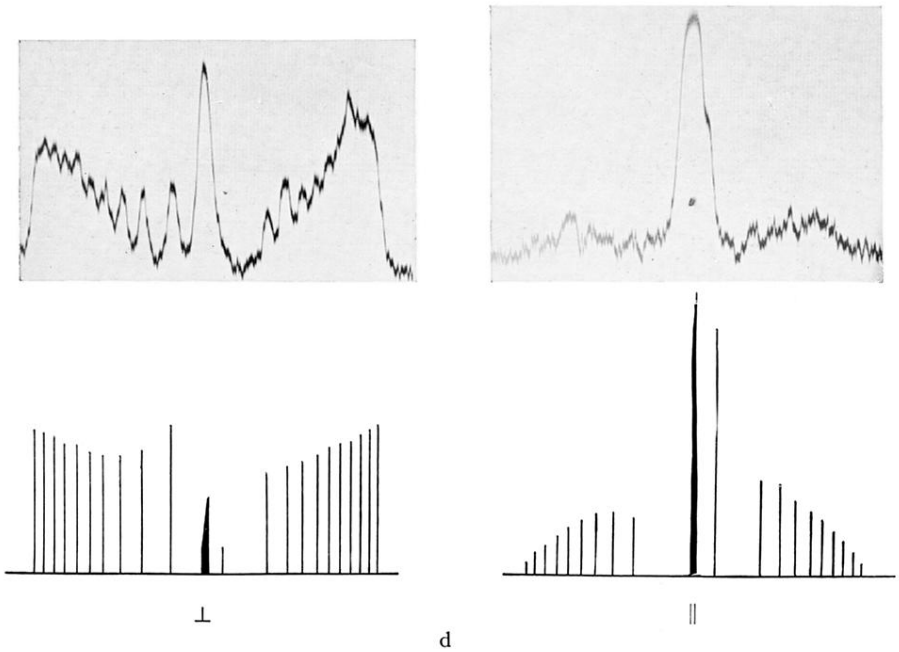

d

Fig. 1. (c). λ5719 Bi II 32500 gauss second order. (d). λ5719 Bi II 43350 gauss second order.

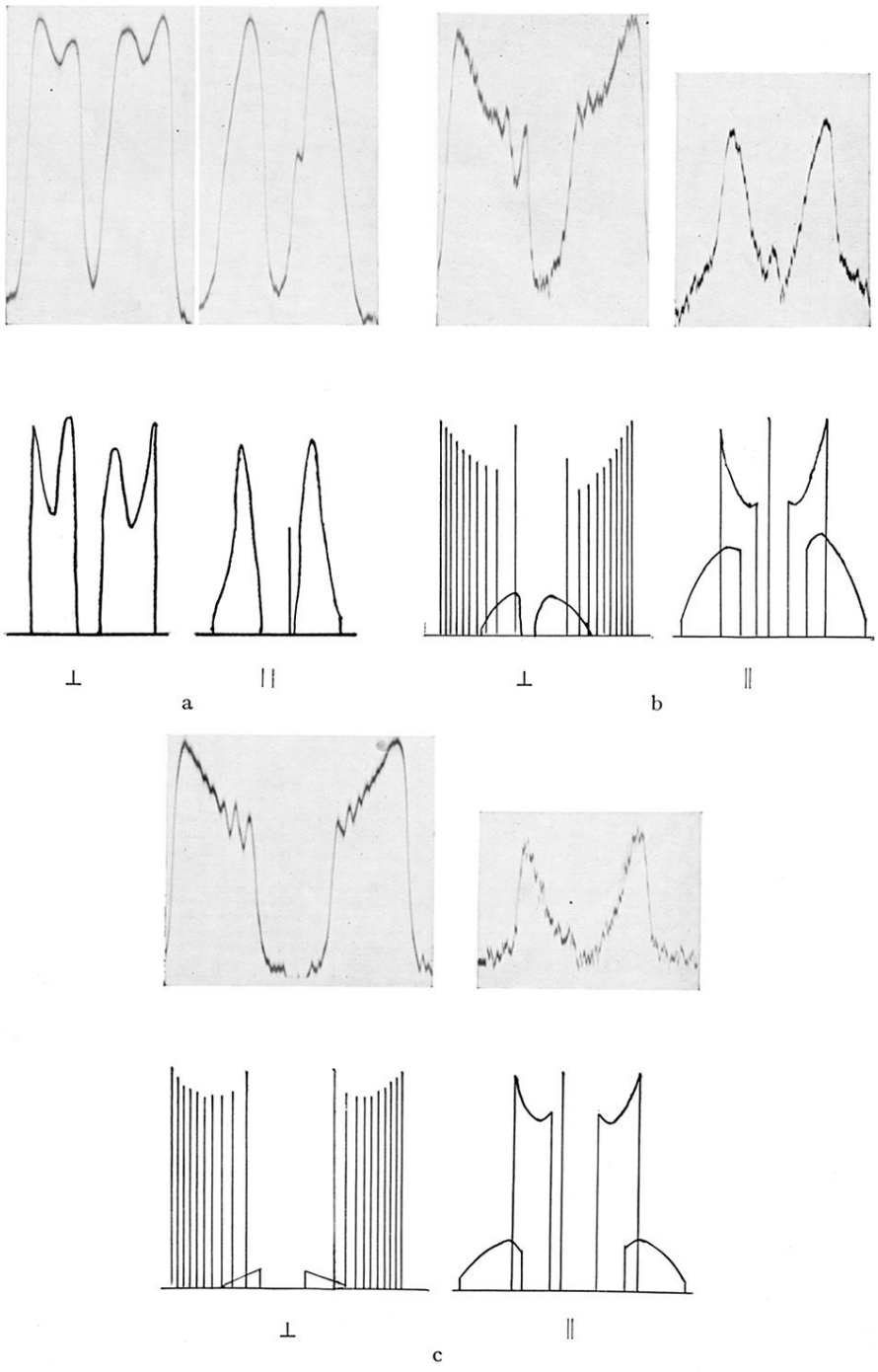

Fig. 2. (a). λ4561 Bi III 14700 gauss second order. (b). λ4561 Bi III 32500 gauss second order. (c). λ4561 Bi III 43350 gauss second order.

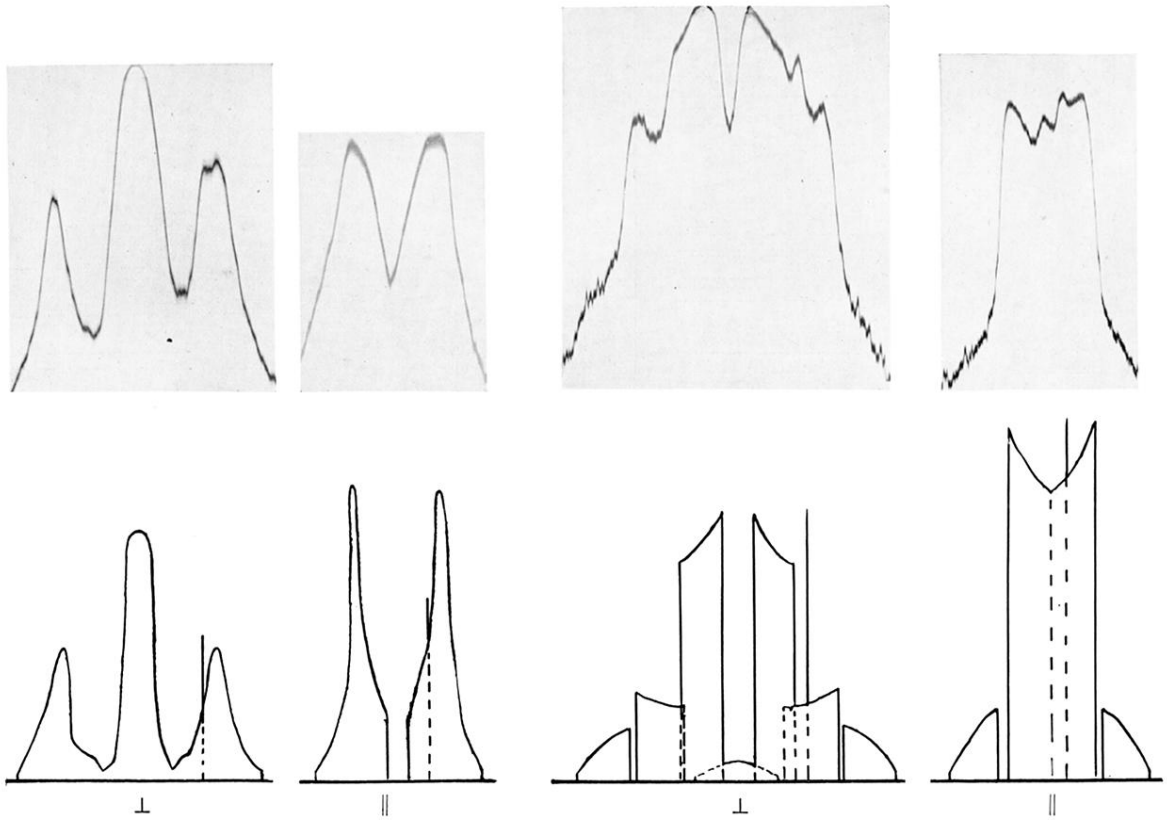

Fig. 3 (a). λ3695 Bi III 14700 gauss third order. (b). λ3695 Bi III 32500 gauss third order.

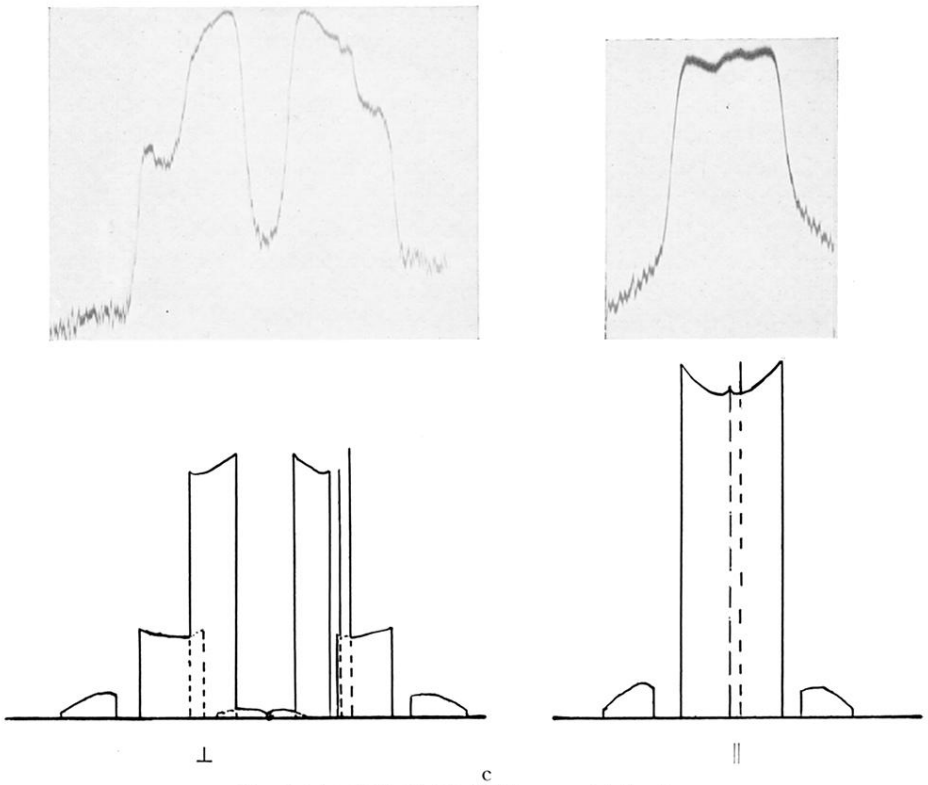

Fig. 3 (c). λ3695 Bi III 43350 gauss third order.